2024 AIAA DATC/IEEE 43rd Digital Avionics Systems Conference (DASC), 29 September - 3 October 2024, San Diego, CA, USA
DOI: 10.1109/DASC62030.2024.10749637

Advanced Mobility Flight Dynamics Restriction to Support High Availability Communication Systems

Fatima Alhashmi
School of Aerospace, Transport and Manufacturing
Cranfield University
f.alhashimi@cranfield.ac.uk

Saba Al-Rubaye
School of Aerospace, Transport and Manufacturing
Cranfield University
s.alrubaye@cranfield.ac.uk

Antonios Tsourdos
School of Aerospace, Transport and Manufacturing
Cranfield University
a.tsourdos@cranfield.ac.uk

***Abstract*— Electric Vertical Take-Off and Landing (eVTOL) platforms play a crucial role in Advanced Air Mobility (AAM) initiatives, particularly in urban environments. Ensuring the safety and reliability of communication networks during air traffic operations is paramount, with communication performance heavily reliant on antenna radiation characteristics. Maintaining consistent communication throughout the entire flight is essential for flight success. However, dynamic maneuvers such as banking turns can result in airframe shadowing, where the vehicle's structure obstructs antenna signals, posing a challenge to communication reliability. This paper proposes a model integrated into eVTOL avionics to mitigate airframe shadowing issues and maintain optimal communication availability during normal flight operations. A new algorithm is proposed, and simulation studies analysis are conducted to assess the impact of airframe shadowing on eVTOL communication performance. Additionally, insights are provided to air traffic management (ATM) and pilots regarding optimal look angles to minimize or avoid airframe shadowing effects.**

Keywords*— *Advanced Air Mobility (AAM), Airframe shadowing, Antenna Look Angle, eVTOL, Link Budget Analysis, Quality of Service (QoS), Satellite communications.

I. INTRODUCTION

Advanced Air Mobility (AAM) is an emerging discipline that aims to create air transportation systems that can be seamlessly incorporated into urban settings, offering quicker, more efficient, and eco-friendly transportation alternatives [1]. Air mobility includes the utilization of various aircraft, such as helicopters, tilt-rotors, and electric vertical take-off and landing (eVTOL) vehicles. To transporting passengers and cargo inside urban regions eVTOL aircraft have received a considerable interest in recent years as a vital facilitator of AAM [2], offering a more environmentally friendly mode of transportation and expediting the development of intelligent cities. Flying eVTOLs in urban environments presents safety risks for passengers, pedestrians, and building components, thereby highlighting the importance of prioritizing safety concerns. To ensure safe functioning of eVTOLs, it is necessary to analyze their requirements for communication, networking, and computing. Airframe shadowing is one of the flight dynamics restrictions occurs when air vehicle performs certain maneuvers which result blockage of the line-of-sight (LOS) component with the communication antenna [3] of aircraft of receiving data from transmitter communication end due to the vehicle body, which affect the quality of transferred radio signals [4]. Most of the existing literature in context of airframe shadowing involve real-world measurements by conducting several measurement campaigns. These measurements consider the size and configuration of the platform, together with the operation frequency. These investigations [5], [6] involved conducting a targeted flight scenario in a chosen region to gather accurate observations regarding the incidence of aircraft shadowing, Fig.1 shown air-to-ground (A2G) communication channels.

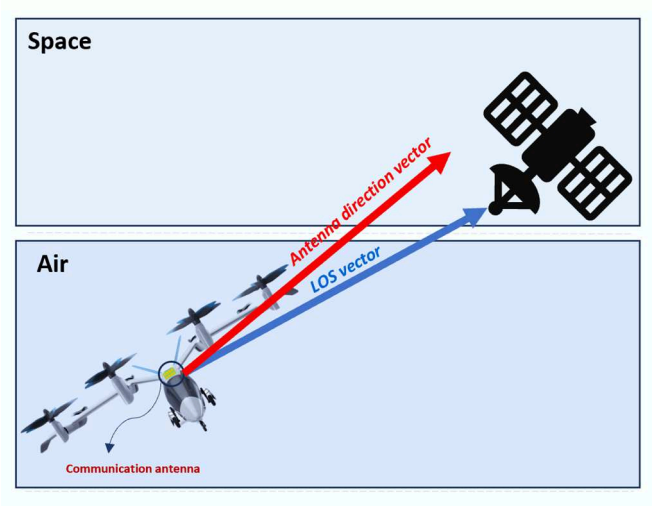

FIGURE: 1AIR COMMUNICATION LINK ELEMENTS

Thus, it was a synthesis of measurement efforts and offered models, the researcher developed a stochastic model to represent airframe shadowing and suggested the potential effectiveness of a deterministic model [7]. Moreover [8] and [9] investigated this in more detail. Multiple UHF and L-band channel measuring campaigns in the airport region were used to examine path-loss and airframe shadowing loss [10]. In summary, researchers have proposed the following four strategies to address the challenges of airframe shadowing: measurement campaigns, stochastic models, path loss models, and semi-deterministic airframe shadowing models. It has been observed that most of the existing research [11], [12] has focused on the air-to-ground communication channel, while the air-to-air channel remains largely unexplored. The main paper contributions, in addition to existing studies, are the following:

1) Introduce novel approach by developing new algorithms aiming to optimize communication during dynamic flight dynamic flight scenarios and establish reliable communication links, enhancing the performance of aircraft communication systems [13].
2) Utilize simulation models that are specifically designed to reduce the negative effects of airframe shadowing on eVTOLs operating in air-to-space communication channels.

3) This research makes a valuable contribution to enhancing the safety and reliability of aviation systems, particularly for eVTOL configurations, by suggesting innovative methods that consider flight dynamics and communication channel propagation.

II. TECHNICAL BACKGROUND

A. AAM Communications

The AAM communication system infrastructure contains air vehicle platforms, including eVTOLs, equipped with communication antennas that interface with various segments ground, air, and space [14]. These connections extend to ground stations, network cell towers, air traffic management (ATM), and satellite communications (SATCOM) [15], involving satellites in different orbits such as Geostationary Earth Orbit (GEO), Medium Earth Orbit (MEO, and Low Earth Orbit (LEO) [16]. Establishing a clear and robust communication infrastructure is crucial in UAM to avoid dangerous accidents and ensure the continuous flow of essential data transmission. In the context of aircraft communication systems, the aircraft and ground station or satellite can interchangeably act as the sender and receiver, working in accordance with specified protocols and frequency bands to facilitate effective communication. The transmission medium is typically wireless, utilizing the air as a conduit for data transfer. Essential elements for establishing communication, including sender, receiver, message content, transmission medium, and protocol. These elements together provide the transfer of crucial control commands and voice data, underscoring the vital role of well-designed communication systems in the safe and efficient operation of AAM [17].

The availability of satellite communication depends on the used orbit, different application used different satellite orbits depend on virous factors transmitter [18]. LEO, MEO, and GEO are the three most common orbits for communication satellites. The respective altitude ranges for LEO, MEO, and GEO are 500 km to 1,000 km, 5,000 km to 12,000 km, and 36,000 km the different satellite types are located in different altitudes around Earth [19], [20]. Moreover, radio communication and specifically satellite communications using radio channels between the aircraft and satellite are conducted over a wide range of frequency bands. Aircrafts utilize antennas of various shapes and sizes. Therefore, study the shapes and sizes of various antennas in aircraft is important to establish communication with the transmitter end in space or ground. Most aircraft are equipped with an upper and a lower antenna for communications frequencies, which allows communication with a ground station, satellite, or another aircraft regardless of the aircraft's orientation [21]. The positioning of antennas is determined by their intended function in aircraft design phase [22].

B. Factors Affect Aircraft Communication Performance

Several factors can affect aircraft communication performance, such as weather, atmospheric conditions, climate changes, doppler shift, antenna orientation, channel capacity, system redundancy, and link resilience [23]. The satellite communication with ground station, satellite, and orbit are synchronized to facilitate seamless data communication. Moreover, monitoring the signal attenuation level from the satellite as it traverses free space and approaches ground structures is essential. Furthermore, flight dynamics which is the science of air-vehicle direction and control in three dimensions, which is the focus scope of this research paper, especially the airframe shadowing problem. While these issues are typically addressed in planned routes of commercial flights, they become crucial challenges in future or unrouted planned flights. These challenges necessitate careful consideration; therefore, that pilots can avoid potential flight maneuvers that might lead to communication problems [24].

C. Flight Dynamics Restrictions

Several flight dynamics restrictions affect communication performance, such as airframe shadowing, sharped maneuvers and antenna look angle. Furthermore, all these factors are indeed related to each other.

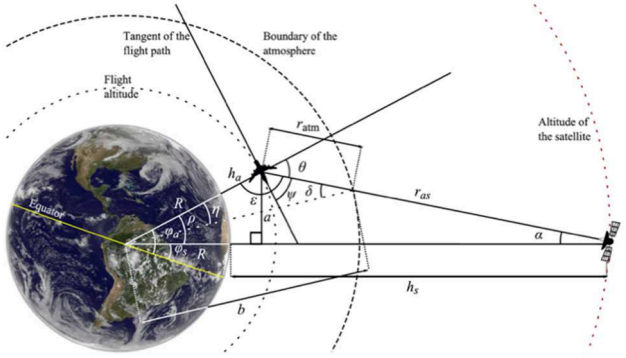

FIGURE 2: THE AIRCRAFT ANGLES AND DISTANCES TO THE SATELLITE COMMUNICATION LINK SYSTEM GEOMETRY [16].

Starting with the antenna look angle, which is also known as the pointing angle from the satellite to other communication as shown aircraft on air as shown in Fig 2. Look angles are combinations of azimuth and elevation angles. Both angles are used to point at the satellite directly from the earth station antenna to maintain the maximum gain of the earth station antenna. Moreover, the azimuth angle is defined as the angle between the local horizontal plane and the plane passing through the satellite, earth station, and center of the earth. While the elevation angle is defined as the angle between the vertical plane and the line pointing to the satellite [25]. Moreover, when the aircraft performed sharp maneuvers can affect the communication performance since the look angle of antenna misalignment the line-of-sight connection with satellite.

D. Airframe Shadowing

Airframe shadowing is influenced by a combination of factors including frequency, flight scenarios, aircraft and antenna locations, and aircraft size. Understanding and accounting for these factors are essential for designing effective communication systems for aircraft, especially for ensuring reliable connectivity in various operating conditions. Airframe shadowing affect the quality of transferred radio signals. which can occur in either air-to-air or also can called air-to-space or air-to-ground links, depending on which structural element, either from the fuselage or wing of the aircraft, blocks the antenna from receiving signals [26]

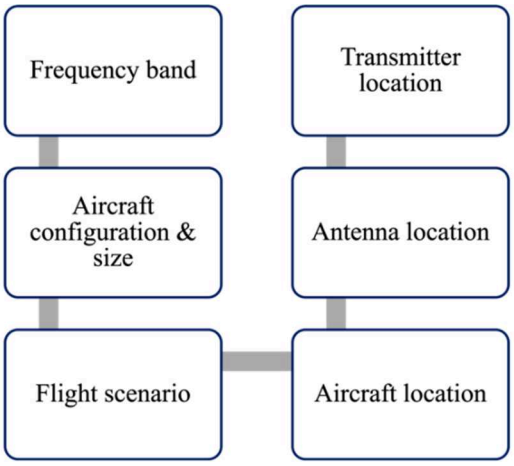

FIGURE 3: AIRFRAME SHADOWING PHENOMENON

As shown in Fig.3 the airframe shadowing phenomenon occurs between the ground station and the aircraft due to the wing, which blocks the antenna depicted in blue located at the bottom of the aircraft, resulting in a signal attenuation. It explains how the aircraft body can form a shadow over the communication antenna, thereby affecting the performance of the communication link. For factors related to the receiver side, airframe shadowing can occur in aircraft of various sizes and configurations. This paper focuses on medium-sized aircraft with fixed-wing configurations, such as eVTOLs, since changes in the airframe can influence the shadowing effect. There are three criteria for evaluating the occurrence of airframe shadowing events caused by the 3D rotation of the air vehicle. LOS path blockage by the airframe occurs when the aircraft roll angle is greater than the elevation angle between the transmitter, typically the ground station (GS), and the aircraft. As shown in Fig.4, the antenna radiation will have an impact by airframe shadowing can be caused by the position of the wing or the engine. Moreover, during banking turns, where the LOS route azimuth lies between the transmitter and the platform, airframe shadowing can occur. This happens when the absolute difference in angles also meets the criteria. Specifically, airframe shadowing arises when the angle between the aircraft's direction and the LOS path falls between 6° and 15°. Furthermore, the design and orientation of the antenna influence the direction and amount of the communication signal which influencing the quantity of shadowing that occurs. Starting with the effect of an antenna's radiation pattern, which describes how the signal is dispersed in space, to examine the signal's propagation. A directional antenna may have a narrower beamwidth, thereby reducing shadowing. Compared to a directional antenna, an omnidirectional antenna may have a larger beamwidth, which can increase the likelihood of shadowing. Additionally, an antenna's gain defines how much it amplifies a signal therefore, antenna with the greater gain may be able to overcome some shadowing effects, but it may also be more likely to experience interference. Moreover, the occurrence of airframe shadowing depends on the communication link, whether it is between the satellite or the ground station. Moreover, one final factor to consider the distance between the receiver and transmitter that impact the amount of shadowing that occurs and create different shadowing scenarios [27].

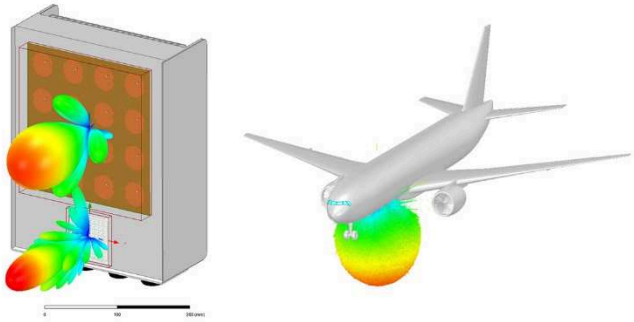

FIGURE 4: ANTENNA RADIATION IMPACT BY AIRCRAFT SHADOW

III. PRPOSED SYSTEM DESIGN

The antennas mounted on the bottom or top of the aircraft can experience blockage due to different aircraft structures. For instance, antennas on the bottom can be impacted by the wings, while those on the top may experience shadowing due to the fuselage or tail.The aerodynamics and control must be considered to analyze the aircraft's response, as they impact the performance of the communication system. The proposed system framework deign of communication systems in aircraft mainly depends on the antenna's radiation properties, as shown in Fig 5. An aircraft's flight dynamics can substantially impact the efficacy and effectiveness of its communication systems. The placement of antennas on an aircraft is a crucial factor, as antennas on the bottom can be affected by the wings, and those on the top by the fuselage or tail.

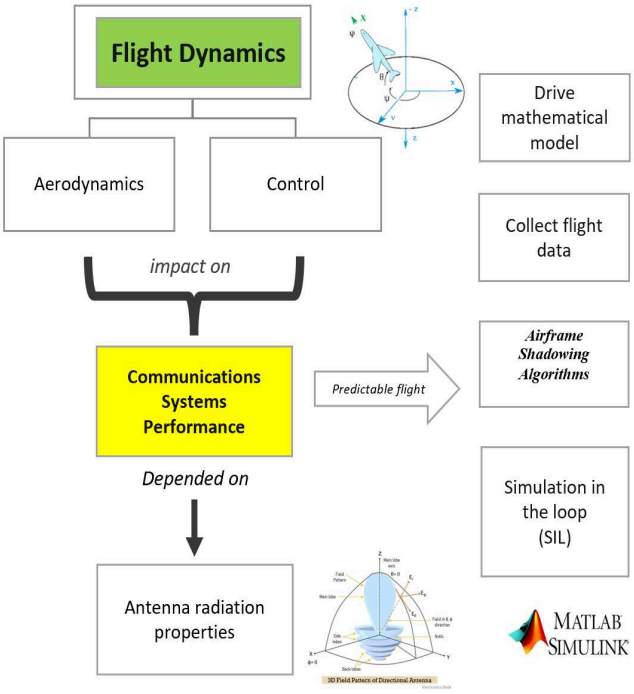

FIGURE 5: AIRCRAFT ROLL ANGLE FOR AIRFRAME SHADOWING EVENT

In addition, antenna characteristics play a significant role in the transmitter side factors causing airframe shadowing. Furthermore, the design and orientation of the antenna influence the direction and amount of the communication signal, thereby affecting the extent of shadowing. Starting with the antenna's radiation pattern, which describes how the signal is dispersed in space, we can examine its impact on signal propagation. A directional antenna, with its narrower beamwidth, can reduce shadowing compared to an omnidirectional antenna, which has a larger beamwidth and can increase the likelihood of shadowing. Additionally, an antenna's gain defines how much it amplifies a signal. An antenna with greater gain may be able to overcome some shadowing effects, but it may also be more susceptible to interference. The occurrence of airframe shadowing also depends on the communication link, whether it is between the satellite or the ground station. Lastly, the distance between the receiver and transmitter is a crucial factor, as it impacts the amount of shadowing and creates different shadowing scenarios.

1) Airframe Shadowing Algorithms

The airframe shadowing algorithm has a dual purpose: first, it detects airframe shadowing events, and second, it provides a solution to mitigate this issue. Initially, the algorithm focuses on developing a detection system for airframe shadowing. Subsequently, it devises a solution to address the problem. This involves presenting a range of optimal look angles to the pilots during flight, ensuring optimal communication performance. Algorithm I illustrate the pseudocode for the proposed system. Firstly, the algorithm extracts various aircraft position maneuvers from the 6DOF data. Then, it proceeds to compute the Quality of Service (QoS) and the link budget of the LOS vector between the satellite and the aircraft. Next, it calculates the LOS vector and look angles for the tested case scenario. The detection of airframe shadowing is implemented by examining the Quality of Service (QoS) matrices [28] and checking for the intersection of the LOS vector with the vehicle body. Upon detection of airframe shadowing, the algorithm quantifies the degree of shadowing and determines a range of look angles for such cases. Conversely, if airframe shadowing is not detected, the model identifies the available look angles while maintaining a LOS connection.

Finally, considering the shadowing data and communication constraints, the algorithm suggests specific angles that pilots should avoid ensuring reliable communication. This ensures optimal communication performance throughout different flight scenarios. Furthermore, the visualization of concept used in the simulation illustrated in algorithm 1. In case one, a high Carrier-to-Noise Ratio (CNR) value is depicted, indicating reliable communication without airframe shadowing. Conversely, in case two, when the aircraft executes certain maneuvers causing a loss of LOS with the satellite, the QoS metrics degrade. This degradation is represented by the loss of LOS between the aircraft and the satellite.

ALGORITHM 1: AIRFRAME SHADOWING MODEL FOR AIRCRAFT

Set the location of the antenna on the Aircraft

Input: *Aircraft position & maneuvers (Pitch θ, Roll ϕ, Yaw ψ) with and without airframe shadowing*

1 *Calculate the **link budget** for the LOS link between the satellite and the aircraft*
2 *Calculate the **QoS** for the LOS link between the satellite and the aircraft*
3 *Calculate LOS vector and **look angles** for both cases*
4 *Initialization look angles values without maneuver ← ideal case of reliable communication*
5 *Input the look angles values of the maneuver case*
6 ***If** (Degrading QoS && 3D body of aircraft intersect with LOS) **do** //*
7 *Airframe shadowing event detected*
8 *Determine the range of look angles with airframe shadowing*
9 *Calculate the degree of shadowing*
10 ***else do** //*
11 *LOS clear, no airframe shadowing detect*
12 ***end***
13 *Determine angles to avoid by the pilot*

The comparison between these two cases demonstrates the impact of airframe shadowing on communication reliability and highlights the importance of mitigating measures to maintain optimal. When certain aircraft maneuvers obstruct the LOS, it leads to degradation in QoS metrics, as depicted in case two where LOS is lost between the aircraft and the satellite, see Fig. 6. Consequently, the application of the airframe shadowing detection algorithm becomes crucial. Once applied, the algorithm proceeds with analyzing the results and proposing solutions to address the issue.

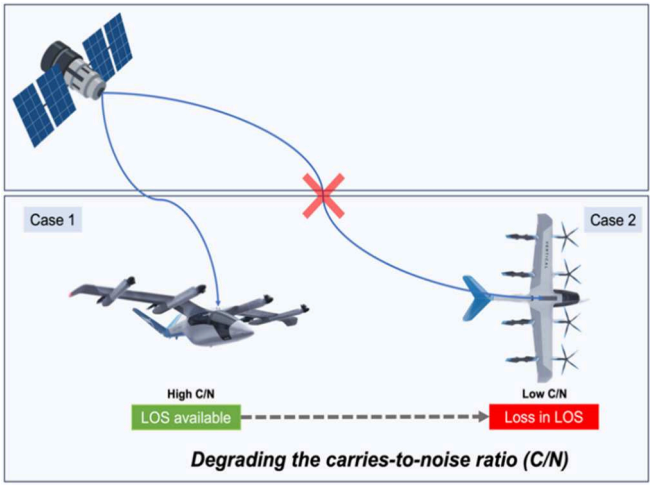

FIGURE 6: DEMONSTRATION FOR POSSIBLE CASES ADDRESSING AIRFRAME SHADOWING ISSUE

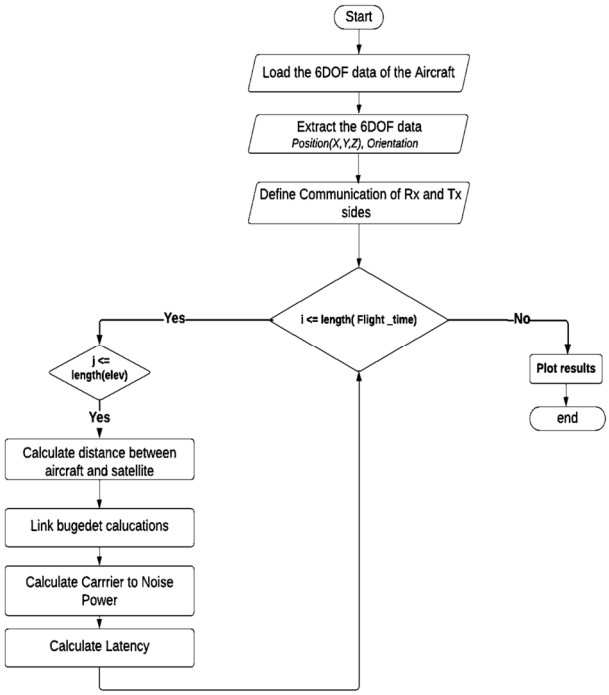

FIGURE 7: FLOWCHART FOR LINK BUDGET AND QOS CODE SECTION

Moreover, two flowcharts, as illustrated in shown in Fig. 7 and Fig. 8 was designed to implement the simulation code in MATLAB. Each flowchart represents a distinct concept implemented in separate simulations. These concepts are then integrated into one main simulation to comprehensively address the complexities associated with airframe shadowing and its impact on communication reliability. By leveraging these flowcharts, the simulation can efficiently analyze various scenarios and evaluate the effectiveness of proposed solutions in mitigating airframe shadowing effects. The flowchart outlines the process of obtaining and processing 6DOF data from the simulation [29]. Initially, the data is saved in MAT file format and then converted to CSV format for easier handling. Communication parameters for both the satellite and aircraft are defined, along with constants required for link budget and QoS calculations. The simulation is structured with nested loops, where the first loop determines the carrier-to-noise ratio threshold, the second loop is time-dependent, and the third loop is based on the elevation angle. Within these loops, link budget and QoS are computed, enabling a thorough assessment of communication performance in various scenarios.

a) Detecting Airframe Shadowing

The airframe shadowing detection algorithm begins by computing the line of sight between the satellite (Tx) and the antenna on top of the aircraft (Rx), generating azimuth and elevation angles for different LOS vectors throughout the flight. Fig. 7, depicts the implementation steps of this algorithm. Starting with the QoS values obtained from previous steps, they are utilized to detect airframe shadowing.

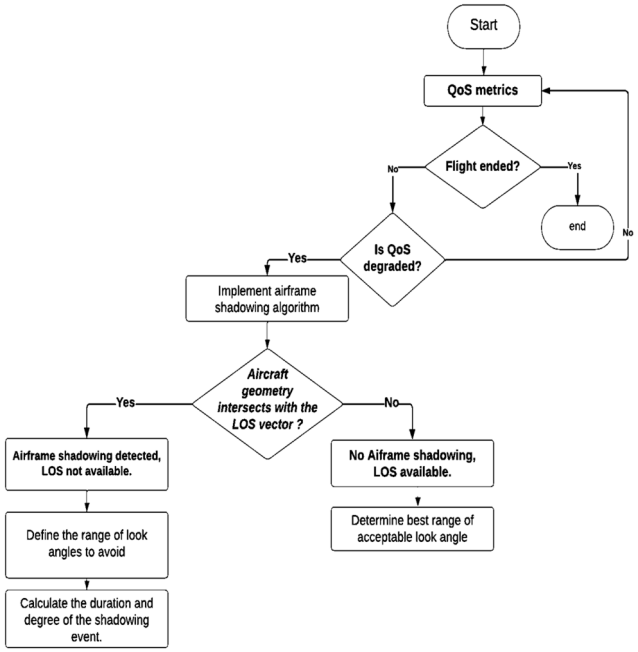

FIGURE 8: AIRFRAME SHADOWING DETECTION FLOWCHART

The algorithm examines the QoS values, and if there's a degradation, it initiates airframe shadowing detection to determine whether the degradation is caused by airframe shadowing or other factors. Airframe shadowing is detected if the 3D model (aircraft geometry) intersects with the LOS, obstructing the signal due to the aircraft's structure. Finally, the algorithm provides look angles for both scenarios, weak and excellent connection, regardless of the presence or absence of airframe shadowing. These angles aid in optimizing communication performance under varying conditions.

IV. SIMULATION AND SCENARIOS

The elements considered in this communication system are satellite and eVTOL. Hence, the simulation only considers the variable parameters associated with the satellite and aircraft while disregarding other features like the ground station. Fig. 9 illustrates the sequential procedures undertaken prior to initiating the simulation. The aircraft model and the airframe configuration model were selected to perform the simulation.

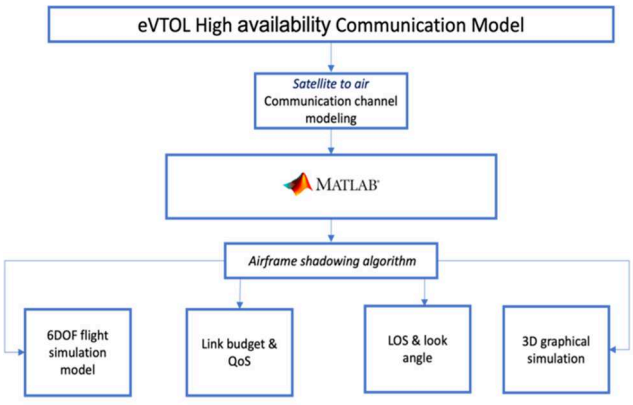

FIGURE 9: SYSTEM SIMULATION STEPS

The aircraft model and the airframe configuration model were selected to perform the simulation. Furthermore, the datasheets defined the communication parameters for the satellite and the aircraft antennas was obtained and used. Afterwards, the flight trajectory, obtained from the six degree of freedom (6DOF) flight simulation, provides real-time position and orientation data, defining the aircraft's 3D geometry to represent the airframe configuration with the antenna locations. Given these details, a complete simulation was developed to address the airframe shadowing issue.

A. Simulation Model Architecture Design

The simulation tool utilized to design and build the system environment. As demonstrated in Fig. 10, the simulation model used in this paper consists of two main components: flight dynamics and wireless communication. Each of these components has its own simulation model script. For the flight dynamics part, the dynamics model was implemented using a 6 Degrees of Freedom (6DOF) flight simulation model.

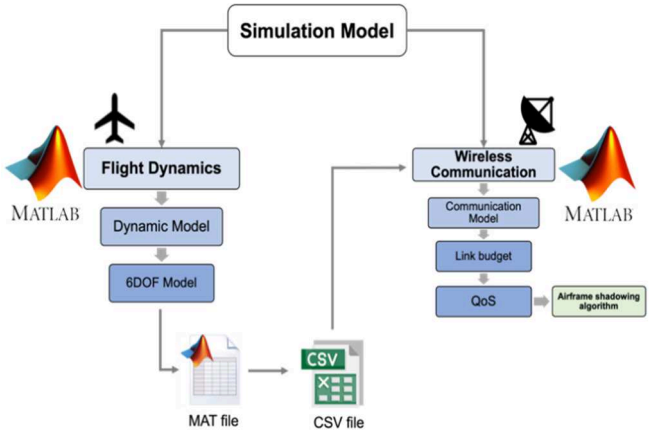

FIGURE 10: SIMULATION ARCHITECTURE DESIGN DIAGRAM

The resulting output of this dynamic model includes the following dynamic states including Position components (x, y, z), Euler angles (roll, pitch, yaw), and Flight time. These data are then stored in a MAT file and converted into a CSV file. The CSV file is subsequently loaded and integrated into the communication model script, where the communication link is evaluated by calculating both the link budget based on the 6DOF data and performing a quality of service (QoS) analysis.

B. Airframe Description and Assumption

Determining an aircraft type and configuration is essential for this research since conducting the study without specifying a platform would be extremely challenging. The simulation has been designed for adaptability to different aircraft configurations by allowing modifications to the 6DOF model, antenna locations, and communication parameters on both the receiver and transmitter sides [31]. This adaptability enables the simulation to be used for a variety of aircraft types and scenarios. The initial assumption was to focus on the VA-X4 eVTOL platform from Vertical Aerospace . However, due to a shortage of publicly available data regarding the aerodynamic configuration of the VA-X4 eVTOL, the aircraft platform was substituted. The new platform used to obtain the dynamic state from the 6DOF flight simulation is a jet aircraft aerodynamic configuration model. The selection of this jet aircraft as the fixed-wing aircraft for this study was based on its specific properties, making it suitable for developing a 6DOF model that could be effectively utilized in the simulation. Although the eVTOL platform differs from the jet aircraft in design, it is important to note that the fixed-wing nature of the jet aircraft is similar to the eVTOL in terms of size and configuration [30].

The link budgeting analysis was employed to assess the communication link performance in the selected scenario, considering various maneuvers and a specific flight trajectory using 6DOF data. Additionally, the main objective of performing a link budget analysis is to assess the dependability of the communication link between eVTOL and the satellites. This is achieved by calculating the gains and losses encountered throughout the system and determining if the power gain is sufficient to establish a successful connection. The following calculations based on the equations and the communication parameters for both the Tx and Rx sides summarized in table I.

TABLE I. PARAMETER OF TX AND RX

Link budget Parameters		
Parameters	**Satellite (Tx)**	**eVTOL/Aircraft (Rx)**
Frequency (Hz)		30×10^9
EIRP (dB)	25	53.5
Gain (dBi)	16.1	47.5
Antenna Diameter (m)	0.65	-
Data rate (Mbps)	50	-
Tilt angle range (deg)	0 *to* 85	-
Bandwidth (Hz)	1×10^9	-
Aperture efficiency (TAE)	~0.68	-
Antenna Input power (W)	-	175
Elevation Range(deg)	[90 − *tilt angle*]	-

C. Antenna Look Angles Determination

The look angle calculations will be adjusted to consider the aircraft's antenna in relation to the GEO satellite, as resisted to the fixed position of the receiver side. Moreover, the aircraft acts as the receiver and moving, implying that its position and orientation change over time. Conversely, the GEO satellite remains stationary in its orbit. This approach simplifies the problem based on the following assumption the Earth is modeled as a perfect spheroid. First, since the location of the satellite is given in the geodetic coordinate system, the LLA (longitude, latitude, Hight) frame is converted into an ECEF frame using the following MATLAB built-in function in the *"Aerospace Toolbox"* as follows:

$$SatPos_{\mathrm{ECEF}} = lla2ecef(SatPos_{lla})$$

Therefore, both the satellite and the aircraft are in the same ECEF frame. The LOS vector as shown in Fig. 11 is obtained between the aircraft and the satellite by

subtracting the aircraft position vector, as illustrated in the yellow point, and the satellite position vector, represented in the red point.

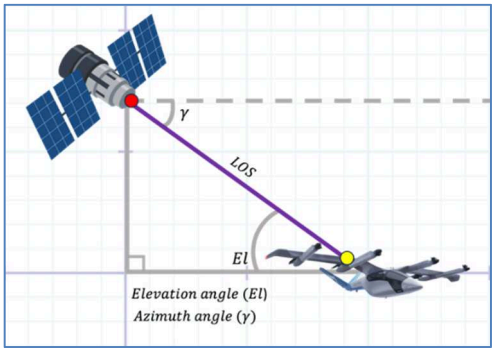

FIGURE 11: LOS VECTOR BETWEEN SATELLITE AND THE ANTENNA ON TOP OF AIRCRAFT WITH LOOK ANGLES

Therefore, the LOS vector in ECEF frame is as follows:

$$\text{LOS}_{\text{ecef}} = \begin{bmatrix} x_{\text{satellite}} - x_{\text{aircraft}} \\ y_{\text{satellite}} - y_{\text{aircraft}} \\ z_{\text{satellite}} - z_{\text{aircraft}} \end{bmatrix} \quad (23)$$

Subsequent, several rotations must be conducted for the LOS vector to reach the antenna body frame, starting by rotating the LOS vector from the ECEF frame to the NED frame, as shown in Fig. 12.

FIGURE 12: THE STEPS OF FRAMES CONVERSION FOR LOOK ANGLES CALCULATIONS

To find the direction of the satellite from the aircraft perspective the LOS vector rotates from ECEF frame to NED frame using DCM [29] as follow:

$$R_{\text{roll}} = \phi = \begin{bmatrix} 1 & 0 & 0 \\ 0 & \cos(\text{Roll}) & -\sin(\text{Roll}) \\ 0 & \sin(\text{Roll}) & \cos(\text{Rolll}) \end{bmatrix} \quad (24)$$

$$R_{\text{pitch}} = \theta = \begin{bmatrix} \cos(\text{Pitch}) & 0 & \sin(\text{Pitch}) \\ 0 & 1 & 0 \\ -\sin(\text{Pitch}) & 0 & \cos(\text{Pitch}) \end{bmatrix} \quad (25)$$

$$R_{\text{yaw}} = \psi = \begin{bmatrix} \cos(\text{Yaw}) & -\sin(\text{Yaw}) & 0 \\ \sin(\text{Yaw}) & \cos(\text{Yaw}) & 0 \\ 0 & 0 & 1 \end{bmatrix} \quad (26)$$

$$\text{DCM} = R_{\text{yaw}} \times R_{\text{pitch}} \times R_{\text{roll}} \quad (27)$$

$$= \begin{bmatrix} \cos\theta\cos\psi & \cos\theta\sin\psi & -\sin\theta \\ \sin\phi\sin\theta\cos\psi & \sin\phi\sin\theta\sin\psi & \sin\phi\cos\theta \\ -\cos\phi\sin\psi & +\cos\phi\cos\psi & \\ \cos\phi\sin\theta\cos\psi & \cos\phi\sin\theta\sin\psi & \cos\phi\cos\theta \\ +\sin\phi\sin\psi & -\sin\phi\cos\psi & \end{bmatrix}$$

Hence, the LOS vector in the NED frame is derived as follows:

$$\text{LOS}_{\text{NED}} = \text{DCM}^T \times \text{LOS}_{\text{ecef}} \quad (28)$$

Next, Rotate the LOS vector from NED frame to aircraft body frame using the built-in function in MATLAB:

$$\text{DCM}_{\text{ned2body}} = \text{eul2dcm}(\text{roll}, \text{pitch}, \text{yaw})'$$

Therefore, the LOS vector in the aircraft body frame is derived as follows. Finally, the last rotation is obtained for the antenna body frame as follows:

$$DCM_{\text{body2antenna}} = \begin{bmatrix} \cos(el_{\text{antenna}}) \cdot \cos(az_{\text{antenna}}) & \cos(el_{\text{antenna}}) \cdot \sin(az_{\text{ant}} \\ -\sin(az_{\text{antenna}}) & \cos(az_{\text{antenna}}) \\ \sin(el_{\text{antenna}}) \cdot \cos(az_{\text{antenna}}) & \sin(el_{\text{antenna}}) \cdot \sin(az_{\text{ant}} \end{bmatrix} \quad (27)$$

$$LOS_{\text{antenna}} = DCM_{\text{body2antenna}} \times LOS_{\text{body}} \quad (28)$$

Thus, the computation of the look angles (azimuth and elevation angles) is performed in the antenna body frame as follows:

$$\gamma\text{=Azimuth}_{\text{antenna}} = \tan^{-1}\left(\frac{\text{LOS}_{\text{antenna (2)}}}{\text{LOS}_{\text{antenna (1)}}}\right) \quad (30)$$

$$\text{El=Elevation}_{\text{antenna}} = \tan^{-1}\left(\frac{\text{LOS}_{\text{antenna (3)}}}{\sqrt{\text{LOS}^2_{\text{antenna (1)}} + \text{LOS}^2_{\text{antenna (2)}}}}\right) \quad (31)$$

V. RESULTS AND ANALYSIS

To accurately reproduce desired maneuvers, it's essential to consider factors beyond just roll, pitch, and yaw rates. Angle of attack, flight path angles, and other elements play crucial roles in influencing aircraft movement.

TABLE II: DYNAMIC STATE DATA FROM 6DOF MODEL FOR CASE STUDY

Time (sec)	Position components			Euler angles		
	X (m)	*Y (m)*	*Z (m)*	*roll ϕ (rad)*	*pitch θ (rad)*	*Yaw ψ (rad)*
1	0	0	-3050	0	4.853	0
2	98.455	0	-3050.27	0	6.344	0
3	196.604	0	-3051.79	0	6.623	0
4	294.373	0	-3054.26	0	7.334	0
5	391.650	0	-3057.68	0	7.818	0
6	488.361	0	-3061.91	0	8.303	0
7	584.438	0	-3066.83	0	8.698	0
8	679.832	0	-3072.32	0	9.024	0
9	774.512	0	-3078.22	0	9.266	0
10	868.461	0	-3084.40	0	9.423	0
11	961.682	0	-3090.70	0	9.492	0
12	1054.191	0	-3096.98	0	9.471	0
13	1146.021	0	-3103.10	0	9.364	0
14	1237.214	0	-3108.93	0	9.172	0
15	1327.829	0	-3114.34	0	8.900	0
16	1417.929	0	-3119.23	0	8.555	0
17	1507.590	0	-3123.49	0	8.146	0
18	1596.891	0	-3127.05	0	7.68	0
19	1685.918	0	-3129.83	0	7.175	0
20	1774.758	0	-3131.802	0	6.636	0

In the case of no airframe shadowing, with the aircraft being a Jet Trainer Aircraft, the given parameters are Aircraft Altitude: 3050 meters and Aircraft Velocity around 0.3. At an altitude of 3050 meters and a velocity corresponding to mach 0.3, the aircraft's speed would be approximately 102.15 meters per second (assuming standard atmospheric conditions). This velocity is about 30% of the speed of sound at sea level. These parameters provide the baseline conditions for analyzing the aircraft's performance and behavior in a scenario without airframe shadowing. In addition The table II presents a subset of the extracted dynamic state data from 6DOF model, showcasing the Carrier-to-Noise Ratio (CNR), QoS, and LOS status at various time intervals during the 30-second simulation.

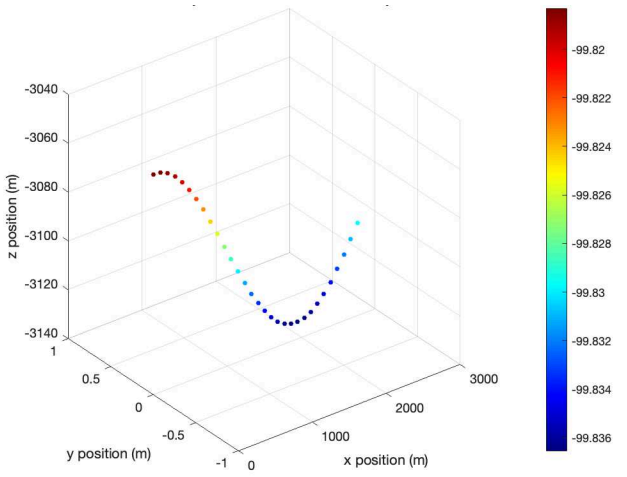

FIGURE 13: DIFFERENT VALUE OF RECEIVED POWER WITH RESPECT TO THE AIRCRAFT POSITION

Fig. 13 display variations in received power as the aircraft maneuvers along its flight path, marked by coordinates X, Y, and Z. A color scale bar shows the received power signal strength (rPdB) at each position, with darker colors indicating lower power zones where reception is poorer. As radio wave propagation principles suggest, received power decreases at higher altitudes due to increased free space path loss from greater distances. Furthermore, the flight path is added in this plot starting from a takeoff altitude as inputted into the simulation model. Similarly, Fig. 14 shows a range of received power from -99.8 dB to -101.2dB for different flight conditions, confirming the accuracy of the power calculations. These values are also influenced by the modulation schemes used in the communication system.

As illustrated in Fig.15 the 3D plot showcases the communication link between the satellite and the aircraft, factoring in the received power along the flight path, as depicted in Fig. 13 The red dot represents the GEO satellite at a fixed altitude around 35000 km, as represented on the z-axis.

In addition, the black dots denote the communication link between the satellite and the aircraft. These dots indicate the presence and reliability of the link between the two communication ends, especially since no airframe shadowing is detected in this scenario. For the airframe shadowing occurrence and analyzing, this plot would visually represent the loss of connection between the satellite and the aircraft.

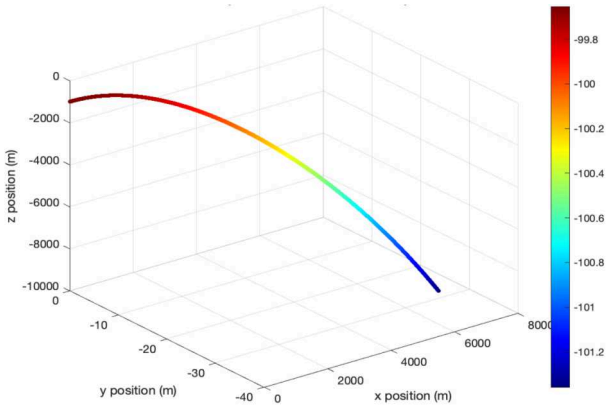

FIGURE 14: DIFFERENT VALUE OF RECEIVED POWER WITH RESPECT TO THE AIRCRAFT POSITION AT DIFFERENT CASE STUDY

Fig. 16 representing the carrier-to-noise ratio values in the unit dB, While, X-axis is representing the elevation angles in degrees, and the Y-axis is representing the time in seconds. Moreover, the different gride color representing different elevation angle. The carrier-to-noise ratio increases, indicating an improvement in signal strength relative to noise. Therefore, offering enhanced communication quality. Furthermore, it is noticeable from the plot that the carrier-to-noise value ranges from -6 dB to 12 dB, an acceptable range considering the characteristics of the Ka-band satcom system and their interaction with atmospheric noises.

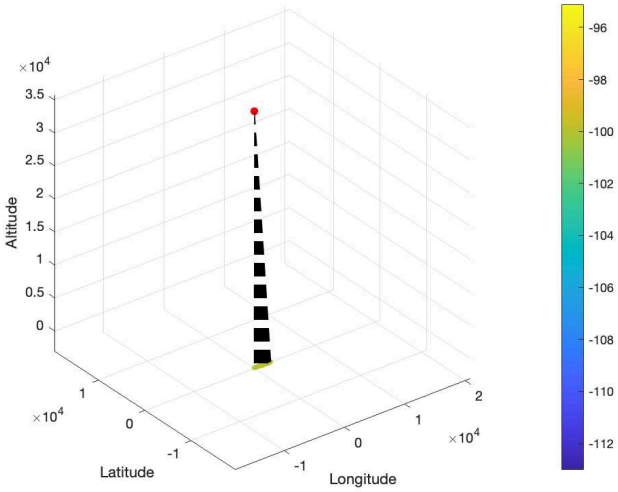

FIGURE 15: 3D VISITATION OF SATELLITE, AIRCRAFT AND RECEIVED POWER

In general, positive C/N values indicate a more reliable and better communication connection. On the other hand, the negative values of C/N indicate a weak communication link. Thus, flights operating at crossbanding altitudes are not advised, even without considering airframe shadowing loss. Fig. 16 provides a broad visualization of the

carrier-to-noise ratio as it changes with both time and elevation angles. The Z-axis denotes the carrier-to-noise ratio in dB unit, while the X-axis showcases the range of elevation angles from 0 to 85 degrees. On the other hand, the Y-axis marks the time in seconds. The varying grid colors in the graph serve as a visual indicator, demonstrating the distinction values to easily determine and compare specific elevation angles with their corresponding carrier-to-noise values at any given time point.

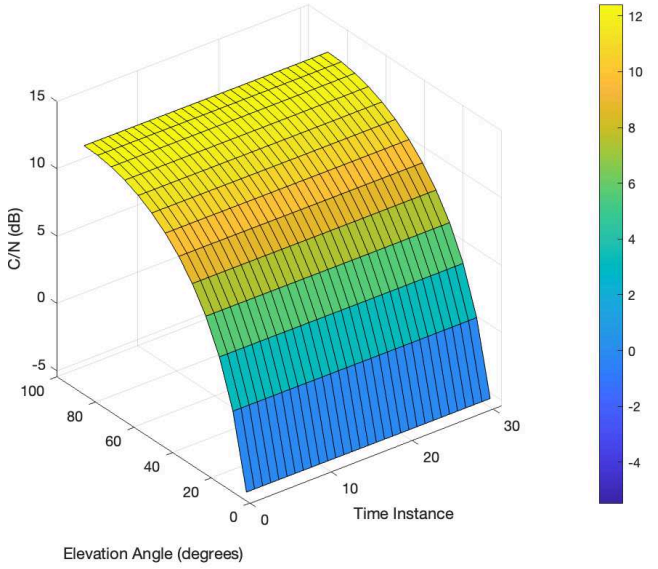

FIGURE 16: CARRIER-TO-NOISE RATION VARYING OVER TIME FOR ELEVATION ANGLE RANGE FROM 0 TO 85 DEGREE

Finally, the simulation outcomes contain measurements about received power, carrier-to-noise ratio, and look angles. The measurements function as threshold values for the specific airframe configuration and satellite, hence enabling the identification of airframe shadowing in comparable situations.

VI. CONCLUSIONS

This paper developed a real-time model for eVTOL avionics that overcomes the dynamic operational limitations of the vehicle under normal flight conditions, aiming to ensure maximum communication availability. A novel methodology was implemented, utilizing a shadowing detection algorithm integrated within a dynamic model simulation. This was conducted in a MATLAB environment, focusing on air-to-space channel modeling between eVTOL communication antennas and a GEO satellite. The algorithm adapted to eVTOL flight dynamics and enhanced the communication system's performance, thereby ensuring reliability in modeled. Furthermore, the simulation identifies flight trajectories and airframe shadowing occurrences, providing pilots with essential guidance on the best communication angles during flights.

VII. ACKNOWLEDGMENTS

This work partially supported by UKRI-EPSRC CHEDDAR Project (Communications Hub for Empowering Distributed Cloud Computing Applications and Research) under grant numbers EP/X040518/1 and EP/Y037421/1, Also, authors would like to thank Thales UK for the kind support.

I. REFFERENCES

[1]. N. Hosseini, H. Jamal, J. Haque, T. Magesacher, and D. W. Matolak, "AV Command and Control, Navigation and Surveillance: A Review of Potential 5G and Satellite Systems.," in IEEE Aerospace Conference, 2019.

[2]. S. Al-Rubaye, A. Tsourdos, and K. Namuduri, "Advanced Air Mobility Operation and Infrastructure for Sustainable Connected eVTOL Vehicle," Drones, vol. 7, no. 5, p. 319, 2023.

[3]. Y. S. Meng and Y. H. Lee, "Study of shadowing effect by aircraft maneuvering for air-to-ground communication," AEU - International Journal of Electronics and Communications, vol. 66, no. 1, pp. 7-11, 2012.

[4]. R. Sun, D. W. Matolak and W. Rayess, "Air-Ground Channel Characterization for Unmanned Aircraft Systems—Part IV: Airframe Shadowing," IEEE Transactions on Vehicular Technology, vol. 66, no. 9, pp. 7643-7652, 2017.

[5]. D. W. Matolak, R. Sun, H. Jamal, and W. Rayess,, "L- and C-band airframe shadowing measurements and statistics for a medium-sized aircraft," in 017 11th European Conference on Antennas and Propagation (EUCAP, 2017.

[6]. Warrier, A.; Al-Rubaye, S.; Inalhan, G.; Tsourdos, A. AI-Enabled Interference Mitigation for Autonomous Aerial Vehicles in Urban 5G Networks. Aerospace 2023, 10, 884. https://doi.org/10.3390/aerospace10100884.

[7]. C. Ge et al., "Pathloss and Airframe Shadowing Loss of Air-to-Ground UAV Channel in the Airport Area at UHF- and L-Band," IEEE Transactions on Vehicular Technology, vol. 72, no. 6, pp. 8094-8098, 2023.

[8]. D. Bonilla Licea, M. Bonilla E., M. Ghogho and M. Saska, "Energy-Efficient Fixed-Wing UAV Relay With Considerations of Airframe Shadowing," IEEE Communications Letters, vol. 27, no. 6, pp. 1550-1554, 2023.

[9]. H. Whitworth, S. Al-Rubaye and A. Tsourdos, "Urban Air Mobility Link Budget Analysis in 5G Communication Systems," 2023 IEEE 24th International Symposium on a World of Wireless, Mobile and Multimedia Networks (WoWMoM), Boston, MA, USA, 2023, pp. 400-406, doi: 10.1109/WoWMoM57956.2023.00071.

[10]. X. Li et al., "Multi-Agent DRL for Resource Allocation and Cache Design in Terrestrial-Satellite Networks," in IEEE Transactions on Wireless Communications, vol. 22, no. 8, pp.

5031-5042, Aug. 2023, doi: 10.1109/TWC.2022.3231379

[11]. X. Liu, H. Zhang, M. Sheng, W. Li, S. Al-Rubaye and K. Long, "Ultra dense satellite-enabled 6G networks: Resource optimization and interference management," in China Communications, vol. 20, no. 10, pp. 262-275, Oct. 2023, doi: 10.23919/JCC.ea.2021-0740.202302.

[12]. Z. Zhou, H. Yu, S. Mumtaz, S. Al-Rubaye, A. Tsourdos and R. Q. Hu, "Power Control Optimization for Large-Scale Multi-Antenna Systems," in IEEE Transactions on Wireless Communications, vol. 19, no. 11, pp. 7339-7352, Nov. 2020, doi: 10.1109/TWC.2020.3010701.

[13]. S. Al-Rubaye, A. Al-Dulaimi and Q. Ni, "Power Interchange Analysis for Reliable Vehicle-to-Grid Connectivity," in IEEE Communications Magazine, vol. 57, no. 8, pp. 105-111, August 2019, doi: 10.1109/MCOM.2019.1800657.

[14]. Y. Gao et al., "Joint Optimization of Depth and Ego-Motion for Intelligent Autonomous Vehicles," in IEEE Transactions on Intelligent Transportation Systems, vol. 24, no. 7, pp. 7390-7403, July 2023, doi: 10.1109/TITS.2022.3159275.

[15]. V. Towhidlou, S. Al-Rubaye and A. Tsourdos, "LTE Handover Design for Cellular-Connected Aircraft," 2022 IEEE/AIAA 41st Digital Avionics Systems Conference (DASC), Portsmouth, VA, USA, 2022, pp. 1-5, doi: 10.1109/DASC55683.2022.9925868.

[16]. J. Kokkoniemi, J. M. Jornet, V. Petrov, Y. Koucheryavy and M. Juntti, "Channel Modeling and Performance Analysis of Airplane-Satellite Terahertz Band Communications," IEEE Transactions on Vehicular Technology, vol. 70, no. 3, pp. 2047-2061, 2021.

[17]. E. Ajanic, M. Feroskhan, V. Wüest, and D. Floreano, "Sharp turning maneuvers with avian-inspired wing and tail morphing," Communications Engineering, vol. 1, no. 1, 2022.

[18]. J. Kunisch , I. de la Torre , A. Winkelmann , M. Eube , and T. Fuss , "Wideband Time-Variant Air-to-Ground Radio Channel Measurements at 5 GHz," in Prpceedings of the 5th European Conference on Antennas and Propagation, Hamburg, 2011.

[19]. A. A. Khuwaja, Y. Chen, N. Zhao, M. -S. Alouini and P. Dobbins, "A Survey of Channel Modeling for UAV Communications," IEEE Communications Surveys & Tutorials, vol. 20, no. 4, pp. 2804-2821, 2018.

[20]. S. Al-Rubaye, C. Conrad and A. Tsourdos, "Communication Network Architecture with 6G Capabilities for Urban Air Mobility," 2024 IEEE International Conference on Consumer Electronics (ICCE), Las Vegas, NV, USA, 2024, pp. 1-6, doi: 10.1109/ICCE59016.2024.10444151

[21]. M. Ozpolat, S. Al-Rubaye, A. Williamson and A. Tsourdos, "Integration of Unmanned Aerial Vehicles and LTE: A Scenario-Dependent Analysis," 2022 International Conference on Connected Vehicle and Expo (ICCVE), Lakeland, FL, USA, 2022, pp. 1-6, doi: 10.1109/ICCVE52871.2022.9742720.

[22]. N. Moraitis and A. D. Panagopoulos, "Coexistence of satellite ground stations in teleport facilities: Interference Assessment, Real Application Scenario and measurements," Sensors, vol. 22, no. 3, p. 1234, 2022.

[23]. Y. He et al., "Two-Timescale Resource Allocation for Automated Networks in IIoT," in IEEE Transactions on Wireless Communications, vol. 21, no. 10, pp. 7881-7896, Oct. 2022, doi: 10.1109/TWC.2022.3162722.

[24]. D. Kosmanos, C. Chaikalis, and I. K. Savvas,, "3GPP 5G V2X Scenarios: Performance of QoS Parameters Using Turbo Codes," Telecom, vol. 3, no. 1, pp. 174-194, 2022.

[25]. S. Mondal, S. Al-Rubaye and A. Tsourdos, "Handover Prediction for Aircraft Dual Connectivity Using Model Predictive Control," in IEEE Access, vol. 9, pp. 44463-44475, 2021, doi: 10.1109/ACCESS.2021.3066554

[26]. A. Warrier, L. Aljaburi, H. Whitworth, S. Al-Rubaye and A. Tsourdos, "Future 6G Communications Powering Vertical Handover in Non-Terrestrial Networks," in IEEE Access, vol. 12, pp. 33016-33034, 2024, doi: 10.1109/ACCESS.2024.3371906. Xx

[27]. H. Whitworth, S. Al-Rubaye and A. Tsourdos, "Utilizing Satellite Communication to Enable Robust Future Flight Data Links," 2023 IEEE/AIAA 42nd Digital Avionics Systems Conference (DASC), Barcelona, Spain, 2023, pp. 1-8, doi: 10.1109/DASC58513.2023.10311102.

[28]. B. S. Rao, S. K. Satnami, M. V. K. S. Prasad and D. V. V. S. Narayana, "Distributed real time modelling of an aerospace vehicle," International Conference on Computing and Communication Technologies, Hyderabad, India, 2014, pp. 1-6, doi: 10.1109/ICCCT2.2014.7066733.

[29]. H. Whitworth, S. Al-Rubaye, A. Tsourdos, J. Jiggins, N. Silverthorn and K. Thomas, "Aircraft to Operations Communication Analysis and Architecture for the Future Aviation Environment," 2021 IEEE/AIAA 40th Digital Avionics Systems Conference (DASC), San Antonio, TX, USA, 2021, pp. 1-8, doi: 10.1109/DASC52595.2021.9594426.

[30]. L. Chen, W. Shi and Z. Chen, "Research on Damping Performance of Dual Mass Flywheel Based on Vehicle Transmission System Modeling and Multi-Condition Simulation," in IEEE Access, vol. 8, pp. 28064-28077, 2020, doi: 10.1109/ACCESS.2019.2951618.

[31]. El Debeiki, M.; Al-Rubaye, S.; Perrusquía, A.; Conrad, C.; Flores-Campos, J.A. An Advanced Path Planning and UAV Relay System: Enhancing Connectivity in Rural Environments. *Future Internet* 2024, *16*, 89. https://doi.org/10.3390/fi16030089.

Advanced mobility flight dynamics restriction to support high availability communication systems

Alhashmi, Fatima

2024-09-29

Alhashmi F, Al-Rubaye S, Tsourdos A. (2024) Advanced mobility flight dynamics restriction to support high availability communication systems. In: 2024 AIAA DATC/IEEE 43rd Digital Avionics Systems Conference (DASC), 29 September 2024 - 3 October 2024, San Diego, CA, USA
https://doi.org/10.1109/dasc62030.2024.10749637